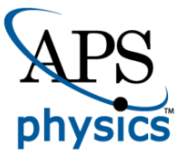

Optical Interferometry with Quantum Networks

E. T. Khabiboulline, J. Borregaard, K. De Greve, and M. D. Lukin

Phys. Rev. Lett. **123**, 070504 — Published 15 August 2019

DOI: 10.1103/PhysRevLett.123.070504

Optical Interferometry with Quantum Networks

E. T. Khabiboulline,[1] J. Borregaard,[1,2] K. De Greve,[1] and M. D. Lukin[1]

[1] *Department of Physics, Harvard University, Cambridge, MA 02138, USA*
[2] *QMATH, Department of Mathematical Sciences, University of Copenhagen, 2100 Copenhagen Ø, Denmark*

We propose a method for optical interferometry in telescope arrays assisted by quantum networks. In our approach, the quantum state of incoming photons along with an arrival time index is stored in a binary qubit code at each receiver. Nonlocal retrieval of the quantum state via entanglement-assisted parity checks at the expected photon arrival rate allows for direct extraction of phase difference, effectively circumventing transmission losses between nodes. Compared to prior proposals, our scheme, based on efficient quantum data compression, offers an exponential decrease in required entanglement bandwidth. Experimental implementation is then feasible with near-term technology, enabling optical imaging of astronomical objects akin to well-established radio interferometers and pushing resolution beyond what is practically achievable classically.

High-resolution imaging using large telescope arrays is by now a well-established technique in the microwave and radio-frequency domains [1, 2]. While extending to the optical domain may offer substantial advantages in terms of resolution [3, 4], this task is extremely challenging in practice. The requirement of interferometric stabilization at optical wavelengths and the weakness of light sources in this domain have precluded the widespread adoption of optical telescope arrays [5]. Notably, the weaker light intensities make phase-sensitive heterodyne detection infeasible due to vacuum fluctuations [6] and high-resolution optical telescopes are therefore operated by directly interfering the collected light [7]. Then, size of the array and consequently resolution is ultimately limited by transmission losses between telescope sites.

In this Letter, we propose a new approach to overcome these limitations with networks [8] of quantum memories connected via entanglement. Specifically, we describe a scheme for efficiently determining the optical phase difference between two widely separated receivers. Each detector runs a "quantum shift register" storing incident photon states at a rate that is matched to the inverse detection bandwidth. Then, at the anticipated mean photon arrival rate, the memories are interrogated with entangled pairs to provide information akin to that obtained from a radio interferometer. Employing quantum repeater techniques [9], this approach completely circumvents transmission losses. The resulting increase in baseline to arbitrarily large distances potentially allows for substantial enhancement in imaging resolution [4].

Before proceeding, we note that the use of entanglement to connect remote telescope sites has been proposed previously, by means of postselected quantum teleportation of incident optical photons [10]. The key limitation of this visionary proposal is the requirement of an excessive amount of distributed entangled pairs. They must be supplied at a rate similar to the spectral bandwidth of the optical telescope, which is currently not feasible. In the relevant case of weak sources, such that incident photons are rare, the use of quantum memories circumvents this requirement. Under distributed compression, the incoming light is efficiently processed using only $\sim\log_2(1/\epsilon)$ memory qubits and entangled pairs, where $\epsilon \ll 1$ is the mean photon number. Then, the entire loss-free interferometric operation can be realized with modest quantum nodes consisting of about 20 qubits and distributed entanglement rate in the 200 kHz range. Our proposal re-

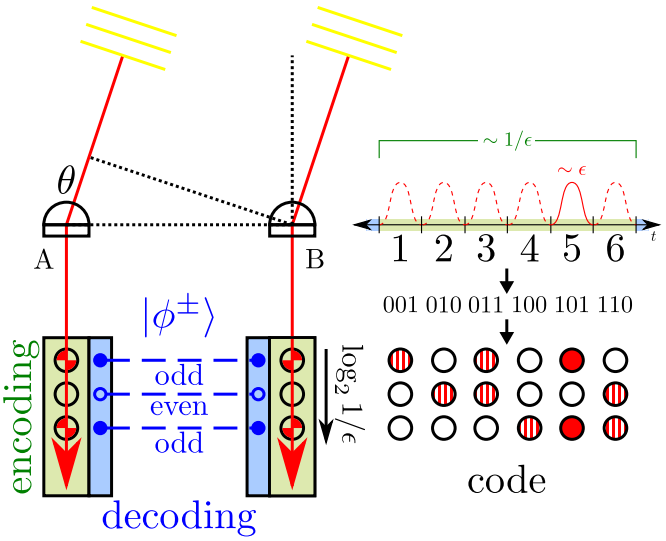

FIG. 1. Overview of basic operation. Light from a distant source is collected at two sites and stored in quantum memory over time bins digitized by detector bandwidth. Both the quantum state and the arrival time of an incident photon are encoded in a binary qubit code. For example, if the photon arrives in the 5th time bin, corresponding to the binary representation 101, we store it in a quantum state with flipped first and third qubits at each node. Decoding of the arrival time is accomplished by nonlocal parity checks assisted by entangled pairs, projecting the memories onto a known entangled state. The phase information can then be extracted without directly interfering the signal from the two memories, thus circumventing transmission losses. Network resources scale only logarithmically with source intensity ϵ.

alizes an effective event-ready scheme, avoiding wasteful expenditure of entanglement for vacuum events.

In our protocol, illustrated in Fig. 1, incoming light is stored by flipping stationary quantum bit memories [11] at each telescope site. The storage procedure operates over a time interval set by the detector bandwidth. Multiple qubits are needed to record a photon spread over many time bins. We assume that the light is weak such that most time bins contain vacuum. Consider, first, a unary encoding with one memory qubit for each time bin. After the single photon is stored, the memories are in a superposition between one site having the excitation versus the other: e.g., $(|000010\ldots\rangle_A |000000\ldots\rangle_B + e^{i\theta} |000000\ldots\rangle_A |000010\ldots\rangle_B)/\sqrt{2}$, where the memory register corresponds to time bin. The goal of the interferometer is to extract the relative phase θ. To determine which memory qubits to use for interferometry without collapsing the superposition, the parity of parallel memory registers can be checked with an entangled state per register. Introducing Bell pairs ($|\phi^{\pm}\rangle = (|0,0\rangle \pm |1,1\rangle)/\sqrt{2}$, where $|i\rangle_A |j\rangle_B \equiv |i,j\rangle$), controlled phase (CZ) gates between the memory qubits on either side and the entangled pairs have the following effect:

$$(|0,0\rangle, |1,1\rangle) |\phi^+\rangle \xrightarrow{2\times \mathrm{CZ}} (|0,0\rangle, |1,1\rangle) |\phi^+\rangle , \quad (1)$$

$$(|0,1\rangle, |1,0\rangle) |\phi^+\rangle \xrightarrow{2\times \mathrm{CZ}} (|0,1\rangle, |1,0\rangle) |\phi^-\rangle . \quad (2)$$

A measurement in the X basis (projecting on the states $|\pm\rangle = (|0\rangle \pm |1\rangle)/\sqrt{2}$) of each qubit in the Bell pair then reveals their parity, from which we can infer arrival time, since the odd-parity register is the one containing the excitation. Its relative phase can be subsequently extracted, e.g., via measurement of one of the qubits in the X basis and the other in a rotated basis to interfere the phase. Similar to a prior scheme [10], the unary code requires one entangled pair for each time bin, implying large consumption for practical bandwidth.

Encoding in binary accomplishes the same task but with a logarithmic scaling of resources. We exploit that only one photon arrives over $M \sim 1/\epsilon$ time bins; i.e., we only have to store one logical qubit per block. Label each time bin $m \in \mathbb{Z}_+$ with its binary representation m_2, and define logical qubits $|\bar{0}\rangle \equiv |0\ldots0\rangle$ and $|\bar{1}_m\rangle \equiv |m_2\rangle$. For example, the 5th time bin is encoded as $|\bar{1}_5\rangle = |1010...0\rangle$, formed from physical qubits at one site. Generally, $\log_2(M+1)$ bits are needed to losslessly encode M possible arrival times plus the vacuum. This encoding is performed by a logical controlled not (CX) gate, which is a product of physical CX gates between the control photonic qubit and target memory qubits specified by the binary representation:

$$|0\rangle (|\bar{0}\rangle, |\bar{1}_j\rangle) \xrightarrow{\overline{\mathrm{CX}}_m} |0\rangle (|\bar{0}\rangle, |\bar{1}_j\rangle) , \quad (3)$$

$$|1\rangle (|\bar{0}\rangle, |\bar{1}_j\rangle) \xrightarrow{\overline{\mathrm{CX}}_m} |1\rangle (|\bar{1}_m\rangle, |\bar{1}_j + \bar{1}_m\rangle) . \quad (4)$$

This encoding keeps track of the arrival time of one photon: empty time bins leave the memories unchanged, whereas only the time bin that does contain a photon maps into the quantum memory via the binary code. Decoupling the photonic qubit through an X-basis measurement completes the encoding step, but imparts a conditional phase associated with each time bin [12]. This phase must be corrected, requiring knowledge of the time bin when the photon did arrive. The arrival time can be decoded while preserving spatial coherence by applying nonlocal parity checks on qubit pairs in the same register, analogously to the case of unary encoding described earlier. For example, if the photon arrived in the 5th time bin, the Bell pairs would be found in the state $|\phi^-\rangle |\phi^+\rangle |\phi^-\rangle |\phi^+\rangle \ldots |\phi^+\rangle$. Since there are $\log_2(M+1)$ qubits per memory, also $\log_2(M+1)$ pre-established entangled pairs are consumed.

Besides identifying the photon arrival time, the parity checks project out the vacuum component of the state. Modeling the astronomical object as a weak thermal source [13, 14], the light arriving in each time bin is described by a density matrix [6]

$$\rho_{AB} = (1-\epsilon)\rho_{\mathrm{vac}} + \frac{\epsilon(1+|g|)}{2} |\psi_\theta^+\rangle \langle\psi_\theta^+| + \frac{\epsilon(1-|g|)}{2} |\psi_\theta^-\rangle \langle\psi_\theta^-| + O(\epsilon^2) , \quad (5)$$

to first order in ϵ, where $|\psi_\theta^{\pm}\rangle = (|0,1\rangle \pm e^{i\theta} |1,0\rangle)/\sqrt{2}$ and $\rho_{\mathrm{vac}} = |0,0\rangle \langle 0,0|$ in the photon-number basis. The first-order spatial coherence $g = |g|e^{i\theta}$, also known as the visibility, generally has amplitude $|g| \leq 1$. The nonlocal parity checks project onto the logical qubit states. After acting on $M \sim 1/\epsilon$ samples of ρ_{AB}, the memories likely contain one logical excitation. This postselection via measurement leads to efficient error accumulation, as elaborated below. The visibility g can then be extracted through a logical measurement, similar to the case of unary encoding discussed above [12].

Specifically, for the example of a photon being detected in the 5th time bin, the memory ends up in the following entangled state up to a known phase flip from the state transfer operation:

$$\frac{(1\pm|g|)}{2} |\bar{\psi}_\theta^+\rangle \langle\bar{\psi}_\theta^+| + \frac{(1\mp|g|)}{2} |\bar{\psi}_\theta^-\rangle \langle\bar{\psi}_\theta^-| , \quad (6)$$

where $|\bar{\psi}_\theta^{\pm}\rangle = (|\bar{0},\bar{1}_5\rangle \pm e^{i\theta} |\bar{1}_5,\bar{0}\rangle)/\sqrt{2}$, which has four entangled physical qubits $(|00,11\rangle \pm e^{i\theta} |11,00\rangle)/\sqrt{2}$. The other, even-parity qubits are in the $|0\rangle$ state and can be traced out. After measuring the first three of the four entangled qubits in the X basis, the remaining qubit is in the state

$$\frac{1}{2} (|0\rangle\langle 0| + |1\rangle\langle 1| + (-1)^{n_-} (g |0\rangle\langle 1| + h.c.)) , \quad (7)$$

where n_- is the number of $|-\rangle$ outcomes from the X-basis measurements. Assume $n_- = 0$ for simplicity. Applying

a phase shift $U_\delta = |0\rangle\langle 0| + e^{i\delta}|1\rangle\langle 1|$ and measuring the qubit in the X basis will have outcome $|\pm\rangle$ with probability $(1 \pm \mathrm{Re}(ge^{-i\delta}))/2$. The visibility g can then be extracted by sweeping over δ, repeating the above procedure for many photons.

Physically, our scheme can be implemented with long-lived atomic ground states in, e.g., Rb atoms [15], using solid-state qubits with an optical interface, such as SiV defect centers in diamond [16–18], or with spin qubits in quantum dots [19], which have fast control. Optical cavities ensure strong light-matter interaction [20], potentially matched via quantum frequency conversion [21]. Absorption of the photon by an auxiliary atom in a Raman setup [22, 23] enables easy X-basis measurement, with the same atom reused for every optical mode. Maintaining a stable phase at the level specified by detector bandwidth can be accomplished with a reference laser, as done in atomic clocks [24]. Logical CX gates between the auxiliary atom and the memory atoms could be realized as cavity-mediated [25] or Rydberg gates [26]. Alternative schemes involve photon-atom gates [11, 27] and photon detection, eliminating the auxiliary atom [21].

The dominant errors in our protocol will arguably originate from the two-qubit gates. Note, however, that all time bins except the one containing the photon will result in trivial CX gates where the control qubit is in state $|0\rangle$. The trivial action of the CX should have an error rate less than $\epsilon(\log_2 1/\epsilon)^{-1}$ to preserve the memory. A number of gate schemes satisfy this criterion [12]; for example, in photon-atom gates, the absence of a photon does not affect the atom. We therefore assume that only the nontrivial CX operations lead to significant errors. We also consider higher-order corrections to the photonic density matrix in Eq. (5), which introduce multiple-photon events leading to undetectable errors in the binary code.

The performance of our scheme is analyzed using the Fisher information, quantifying how much information about a given parameter can be extracted through measurement on a quantum state [28]. In our case, we wish to estimate the visibility $g = g_1 + ig_2$, where g_1, g_2 are two real parameters, so the Fisher information becomes a matrix. Taking the trace norm, $\|F\|$ quantifies the total obtainable information about g: $1/\|F\|$ has the operational interpretation of constraining the variance of the measured data [29]. Ideal nonlocal and local schemes operating on the state of Eq. (5) are separated by $\|F\| \geq M\epsilon$ and $\|F\| \leq M\epsilon^2$, respectively [6]. Intuitively, the nonlocal bound corresponds to the probability of detecting a photon from a source of intensity ϵ, whereas the local bound is a factor of ϵ worse due to the inability to discriminate against the vacuum component of the state. Thus, the Fisher information explicitly demonstrates how nonlocal schemes like ours are superior to local schemes like heterodyne detection for measuring weak thermal light, as found in the optical domain.

Incorporating errors and operating over M time bins,

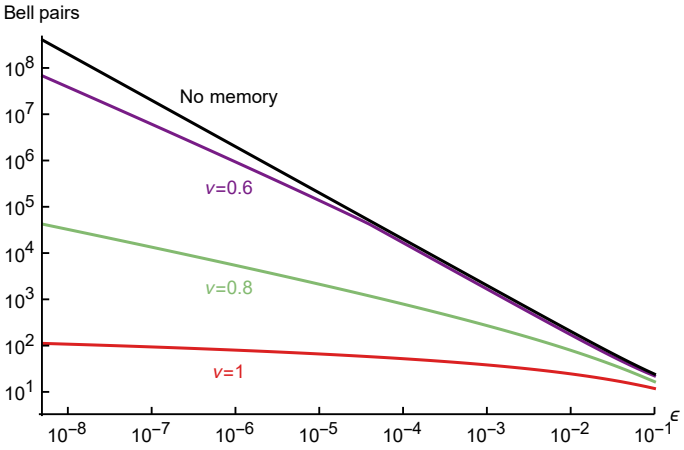

FIG. 2. Minimum number of Bell pairs needed to attain $\|F\| \geq 1$, corresponding to variance $\lesssim 1$ in estimating the visibility g, as a function of source intensity ϵ. We consider errors in the coding operations parametrized by decreasing ν, as detailed in the main text. Ideally ($\nu = 1$), $M \sim 1/\epsilon$ time bins are encoded per block and read out with $\log_2(M+1)$ entangled pairs. For sufficiently large errors ($\nu = 0.6$), the encoding fails and memoryless operation with readout of every time bin is recovered, similar to the scheme of Ref. [10].

we find the following norm of the Fisher information, bounded from below [12]:

$$\|F\| \geq \frac{(M\epsilon)^2}{[(1+\epsilon)^M - 1](1+\epsilon)^{M+2}} \mu^2 \nu^{\log_2(M+1)} \equiv \|F\|_{\min}, \tag{8}$$

where $\mu \equiv p_t(2f_t - 1)^2(2f_1 - 1)^2$ contains the error in mapping the photonic state to memory at one site, in terms of success probability p_t and fidelity f_t of the light-memory transfer and fidelity of one-qubit measurement f_1, and $\nu \equiv (2f_1 - 1)^4(2f_2 - 1)^4(2f_e - 1)$ contains the error of memory encoding/decoding and readout in terms of the fidelities of one-qubit measurements f_1, nontrivial two-qubit gates f_2, and pre-shared entanglement f_e. The success probability includes photon loss, which effectively increases the vacuum component of the state. Other errors are not detectable and modeled as depolarizing channels as a worst-case scenario. Note that $\|F\|_{\min} \sim M\epsilon$ for small ϵ, as expected for a nonlocal scheme. Larger M improves the probability of receiving the signal of a single photon and hence $\|F\|_{\min}$ initially increases, but eventually a maximum is reached due to competition from multiple-photon events and imperfect quantum operations. Therefore, the scheme can be optimized with respect to M, operating with the minimum entanglement expenditure needed to extract the information content of one photon, $\|F\|_{\min} \geq 1$ (see Fig. 2). In the ideal case ($\nu = 1$), the number of entangled pairs is logarithmic in $1/\epsilon$, the number of time bins operated over so that roughly one photon arrives, on average. Information-theoretic arguments, based on the conditional entropy of

the state described by Eq. (5), predict a bound with the same scaling, within a constant prefactor [12]. When errors are sufficiently large ($\nu \approx 60\%$), the memories are read out after a single time bin. Thus, an effective memoryless scheme similar to that of Ref. [10] is recovered, with entanglement consumption scaling as $1/\epsilon$ [30].

Assuming an effective detection bandwidth $\delta_f = 10$ GHz, a total area of photon collection of 10 m^2, and imaging in the V band (centered around 555 nm), we can estimate the resources needed for a star of magnitude 10 (corresponding to $\epsilon = 7\times10^{-7}$), which is around the limit of the CHARA optical interferometric array [31]. Our ideal, optimized scheme requires $\sim\log_2 1/\epsilon \sim 20$ memory qubits per site and an entanglement distribution rate of $\sim\delta_f\epsilon\log_2 1/\epsilon \sim 200$ kHz [32]. The improvement over the rate necessary for a memoryless scheme [10] with the 10 GHz effective bandwidth is a factor of 5×10^4. Extending the current limit of 330 m baseline of CHARA [33] to realistic quantum network scales greater than 10 km would increase resolution from the mas to the μas regime [12]. Finally, we note that the bandwidth of direct interferometers can in practice be adjusted to enhance signal strength at the expense of resolution [33]. While the present method is limited by the bandwidth of quantum memory, our approach readily extends to broadband operation, as discussed in Ref. [21].

Turning to possible implementations of these ideas, we note that the chosen detector bandwidth (10 GHz) sets the timescale of the encoding operation and the photon arrival rate (1 kHz) determines the memory coherence time. In Table I of the Supplement [12], we compare the capabilities of various physical realizations. Among the most promising candidates are SiV centers in diamond, striking a balance with gate time on the order of ns and ms-scale coherence. Techniques such as parallelization, repeated readout, and photon detection [21] improve performance with a modest overhead in resources. Furthermore, we emphasize that our scheme performs well in the presence of noise, which ultimately reduces the interference, as seen in Fig. 2. Therefore, it is amenable to experimental testing and development of Noisy Intermediate-Scale Quantum devices. Demonstrating kHz-scale entanglement generation between remote quantum memories, high-fidelity light-matter interfaces, and addressing of multiple qubits at network nodes would facilitate the realization of our proposal.

In order to image a broad object, telescope arrays consisting of $N > 2$ sites are used to sample the visibility $g(x)$ across $N-1$ points between $x = 0$ and $x = b$ (b is the baseline, or maximum length). According to the Van Cittert-Zernike theorem [34], a Fourier transform yields an estimate of the stellar intensity distribution $I(\phi)$. To operate in this manner, our network protocol generalizes to $N > 2$ nodes. Under conditions when at most one photon is incident on the telescope array, at each site we encode the optical modes in a binary code, as in

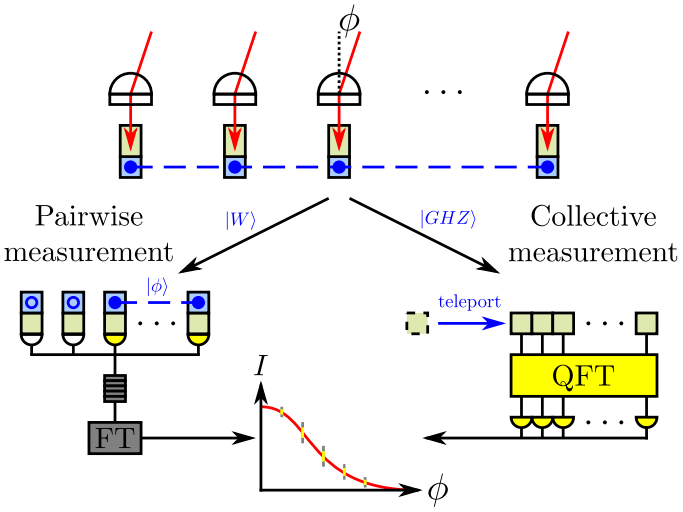

FIG. 3. Generalization to $N > 2$ sites in the telescope array. Decoding with a W state collapses the network state to two nodes, and the protocol continues as before. The visibility data is stored in a classical memory until enough events have accumulated to perform a Fourier transform. Using GHZ states instead preserves coherence across the network. Quantum teleporting the memories to one site for convenience, a quantum Fourier transform is applied, yielding the desired intensity distribution directly as the probabilities of measurement outcomes.

the two-node case. The nonlocal parity checks are performed using either N-qubit GHZ states, preserving coherence across the entire array, or with W states, collapsing the operation into pairwise readout [21]. While a classical Fourier transform of extracted pairwise visibilities may be performed, the GHZ approach enables a quantum Fourier transform directly on the stored quantum state (see Fig. 3). Coherent processing of the visibilities in the latter case results in an additional improvement in the signal-to-noise ratio, since the noise associated with pairwise measurements is avoided. The exact improvement depends on the nature of the source distribution, but can be on the order of $\sqrt{N}$ [21].

In conclusion, we have proposed a protocol for performing nonlocal interferometry over a quantum network, relevant for astronomical imaging. By encoding the quantum state of the incoming photons into memory, we realize an effective "event-ready" scheme with efficient entanglement expenditure. The nonlocality is vital for removing vacuum noise in imaging weak thermal light, and distributed entanglement circumvents transmission losses. Hence, our scheme enables near-term quantum networks to serve as a platform for powerful optical interferometers, demonstrably superior to what can be achieved classically. Furthermore, quantum algorithms can be used to process the stored signals such that the stellar intensity distribution can be inferred with a further improvement in the signal-to-noise ratio.

While we focused on addressing fundamental limitations, real-world interferometry suffers from many other practical challenges such as stabilization and atmospheric phase fluctuations [5], which we address in Table II of the Supplement [12]. For example, in Earth-based systems, atmospheric distortion can be tackled via a combination of adaptive optics and fringe-tracking. Such techniques are already being deployed in smaller-scale astronomical interferometers [3] and are fully compatible with our proposal. Moreover, these challenges and control methods do not scale unfavorably with the baseline beyond certain physical correlation lengths [5], such that the construction of very large telescope arrays may be envisioned. Alternatively, space-based implementation avoids many of these technical issues, potentially extending over the 10^4 km scale [35] using entanglement distributed by satellites [36]. Since the astronomical origin of the weak thermal light is not crucial, such networks could also be applied to terrestrial imaging.

We thank A. Aspuru-Guzik, M. Bhaskar, F. Brandão, M. Christandl, I. Chuang, I. Cirac, J. Stark, C. Stubbs, H. Zhou, and P. Zoller for illuminating discussions and useful comments. This work was supported by the National Science Foundation, the Center for Ultracold Atoms, the NSF Graduate Research Fellowship (E.T.K.), the Vannevar Bush Faculty Fellowship, ERC Grant Agreement no 337603, the Danish Council for Independent Research (Sapere Aude), Qubiz – Quantum Innovation Center, and VILLUM FONDEN via the QMATH Centre of Excellence (Grant No. 10059).

[1] A. R. Thompson, in *Synthesis Imaging in Radio Astronomy II*, Astronomical Society of the Pacific Conference Series, Vol. 180, edited by G. B. Taylor, C. L. Carilli, and R. A. Perley (1999) p. 11.

[2] K. I. Kellermann and J. M. Moran, Annual Review of Astronomy and Astrophysics **39**, 457 (2001).

[3] P. Stee, F. Allard, M. Benisty, L. Bigot, N. Blind, H. Boffin, M. Borges Fernandes, A. Carciofi, A. Chiavassa, O. Creevey, P. Cruzalebes, W.-J. de Wit, A. Domiciano de Souza, M. Elvis, N. Fabas, D. Faes, A. Gallenne, C. Guerrero Pena, M. Hillen, S. Hoenig, M. Ireland, P. Kervella, M. Kishimoto, N. Kostogryz, S. Kraus, A. Labeyrie, J.-B. Le Bouquin, A. Lebre, R. Ligi, A. Marconi, T. Marsh, A. Meilland, F. Millour, J. Monnier, D. Mourard, N. Nardetto, K. Ohnaka, C. Paladini, K. Perraut, G. Perrin, P. Petit, R. Petrov, S. Rakshit, G. Schaefer, J. Schneider, D. Shulyak, M. Simon, F. Soulez, D. Steeghs, I. Tallon-Bosc, M. Tallon, T. ten Brummelaar, E. Thiebaut, F. Thévenin, H. Van Winckel, M. Wittkowski, and J. Zorec, ArXiv e-prints (2017), arXiv:1703.02395 [astro-ph.SR].

[4] T. A. ten Brummelaar, H. A. McAlister, S. T. Ridgway, J. W. G. Bagnuolo, N. H. Turner, L. Sturmann, J. Sturmann, D. H. Berger, C. E. Ogden, R. Cadman, W. I. Hartkopf, C. H. Hopper, and M. A. Shure, The Astrophysical Journal **628**, 453 (2005).

[5] A. R. Thompson, J. M. Moran, and G. W. Swenson, *Interferometry and Synthesis in Radio Astronomy*, 2nd ed. (Wiley-VCH Verlag GmbH, 2007).

[6] M. Tsang, Phys. Rev. Lett. **107**, 270402 (2011).

[7] P. Darré, R. Baudoin, J.-T. Gomes, N. J. Scott, L. Delage, L. Grossard, J. Sturmann, C. Farrington, F. Reynaud, and T. A. ten Brummelaar, Phys. Rev. Lett. **117**, 233902 (2016).

[8] H. J. Kimble, Nature **453**, 1023 (2008).

[9] H.-J. Briegel, W. Dür, J. I. Cirac, and P. Zoller, Phys. Rev. Lett. **81**, 5932 (1998).

[10] D. Gottesman, T. Jennewein, and S. Croke, Phys. Rev. Lett. **109**, 070503 (2012).

[11] S. Ritter, C. Nölleke, C. Hahn, A. Reiserer, A. Neuzner, M. Uphoff, M. Mucke, E. Figueroa, J. Bochmann, and G. Rempe, Nature **484**, 195 (2012).

[12] See Supplemental Material at [URL will be inserted by publisher] for details on the encoding map, derivation of the Fisher information, entanglement resource analysis, overview of technical specifications, and discussion of issues in realistic interferometry, along with Refs. [37–58].

[13] J. Zmuidzinas, J. Opt. Soc. Am. A **20**, 218 (2003).

[14] M. Tsang, R. Nair, and X.-M. Lu, Phys. Rev. X **6**, 031033 (2016).

[15] H. P. Specht, C. Nolleke, A. Reiserer, M. Uphoff, E. Figueroa, S. Ritter, and G. Rempe, Nature **473**, 190 (2011).

[16] C. Wang, C. Kurtsiefer, H. Weinfurter, and B. Burchard, Journal of Physics B: Atomic, Molecular and Optical Physics **39**, 37 (2005).

[17] L. J. Rogers, K. D. Jahnke, T. Teraji, L. Marseglia, C. Müller, B. Naydenov, H. Schauffert, C. Kranz, J. Isoya, L. P. McGuinness, and F. Jelezko, Nature Communications **5** (2014).

[18] A. Sipahigil, K. D. Jahnke, L. J. Rogers, T. Teraji, J. Isoya, A. S. Zibrov, F. Jelezko, and M. D. Lukin, Phys. Rev. Lett. **113**, 113602 (2014).

[19] D. Press, T. D. Ladd, B. Zhang, and Y. Yamamoto, Nature **456**, 218 (2008).

[20] A. Sipahigil, R. E. Evans, D. D. Sukachev, M. J. Burek, J. Borregaard, M. K. Bhaskar, C. T. Nguyen, J. L. Pacheco, H. A. Atikian, C. Meuwly, R. M. Camacho, F. Jelezko, E. Bielejec, H. Park, M. Lončar, and M. D. Lukin, Science **354**, 847 (2016).

[21] See accompanying article at [URL will be inserted by publisher] for extensions of our scheme relevant for a telescope array. We also provide details on the gain from a quantum Fourier transform and realizations of photon-memory state transfer.

[22] J. I. Cirac, P. Zoller, H. J. Kimble, and H. Mabuchi, Phys. Rev. Lett. **78**, 3221 (1997).

[23] A. D. Boozer, A. Boca, R. Miller, T. E. Northup, and H. J. Kimble, Phys. Rev. Lett. **98**, 193601 (2007).

[24] A. D. Ludlow, M. M. Boyd, J. Ye, E. Peik, and P. O. Schmidt, Rev. Mod. Phys. **87**, 637 (2015).

[25] T. Pellizzari, S. A. Gardiner, J. I. Cirac, and P. Zoller, Phys. Rev. Lett. **75**, 3788 (1995).

[26] M. Saffman, T. G. Walker, and K. Mølmer, Rev. Mod. Phys. **82**, 2313 (2010).

[27] T. G. Tiecke, J. D. Thompson, N. P. De Leon, L. Liu, V. Vuletic, and M. D. Lukin, Nature **508**, 241 (2014).

[28] S. L. Braunstein and C. M. Caves, Phys. Rev. Lett. **72**, 3439 (1994).

[29] The Crámer-Rao bound [59] is $\Sigma \geq 1/F$, where Σ is the covariance matrix of the parameters being estimated. Note that $\|\Sigma\| \geq 1/\|F\|$ and the eigenvalues of Σ are the variances along the principal components of the measured data.

[30] A priori, there is a factor of 2 improvement from not having to postselect out half the photon events that do not reveal which-path information; our scheme always preserves coherence between sites. However, this advantage is counterbalanced by multiple-photon and gate errors.

[31] T. A. ten Brummelaar, J. Sturmann, S. T. Ridgway, L. Sturmann, N. H. Turner, H. A. McAlister, C. D. Farringtin, U. Beckmann, G. Weigelt, and M. Shure, Journal of Astronomical Instrumentation **02**, 1340004 (2013).

[32] Due to buildup of error, the optimized block length $1/\epsilon$ of encoded/decoded time bins decreases, by a factor of $(0.7, 0.4, 0.1)$ for $\nu \in (1, 0.8, 0.6)$. Also note that accounting for storing the pre-shared entangled pairs gives another factor of 2 for the memory requirement.

[33] E. Pedretti, J. D. Monnier, T. ten Brummelaar, and N. D. Thureau, New Astronomy Reviews **53**, 353 (2009), proceedings: VLTI summerschool.

[34] F. Zernike, Physica **5**, 785 (1938).

[35] J. D. Monnier, Reports on Progress in Physics **66**, 789 (2003).

[36] J. Yin, Y. Cao, Y.-H. Li, S.-K. Liao, L. Zhang, J.-G. Ren, W.-Q. Cai, W.-Y. Liu, B. Li, H. Dai, G.-B. Li, Q.-M. Lu, Y.-H. Gong, Y. Xu, S.-L. Li, F.-Z. Li, Y.-Y. Yin, Z.-Q. Jiang, M. Li, J.-J. Jia, G. Ren, D. He, Y.-L. Zhou, X.-X. Zhang, N. Wang, X. Chang, Z.-C. Zhu, N.-L. Liu, Y.-A. Chen, C.-Y. Lu, R. Shu, C.-Z. Peng, J.-Y. Wang, and J.-W. Pan, Science **356**, 1140 (2017).

[37] M. Horodecki, J. Oppenheim, and A. Winter, Nature **436**, 673 (2005).

[38] M. Horodecki, J. Oppenheim, and A. Winter, Communications in Mathematical Physics **269**, 107 (2007).

[39] C. Ahn, A. C. Doherty, P. Hayden, and A. J. Winter, IEEE Transactions on Information Theory **52**, 4349 (2006).

[40] I. Bjelaković, H. Boche, and G. Janen, Journal of Mathematical Physics **54**, 032204 (2013).

[41] E. Waks, K. Inoue, and Y. Yamamoto, in *2002 Summaries of Papers Presented at the Quantum Electronics and Laser Science Conference* (2002) pp. 29–30.

[42] J. Borregaard, P. Kómár, E. M. Kessler, A. S. Sørensen, and M. D. Lukin, Phys. Rev. Lett. **114**, 110502 (2015).

[43] R. Stockill, M. J. Stanley, L. Huthmacher, E. Clarke, M. Hugues, A. J. Miller, C. Matthiesen, C. Le Gall, and M. Atatüre, Phys. Rev. Lett. **119**, 010503 (2017).

[44] A. Reiserer, N. Kalb, G. Rempe, and S. Ritter, Nature **508**, 237 (2014).

[45] S. Welte, B. Hacker, S. Daiss, S. Ritter, and G. Rempe, Phys. Rev. X **8**, 011018 (2018).

[46] M. Körber, O. Morin, S. Langenfeld, A. Neuzner, S. Ritter, and G. Rempe, Nature Photonics **12**, 18 (2018).

[47] D. Kim, S. G. Carter, A. Greilich, A. S. Bracker, and D. Gammon, Nature Physics **7**, 223 (2010).

[48] L. Huthmacher, R. Stockill, E. Clarke, M. Hugues, C. Le Gall, and M. Atatüre, Phys. Rev. B **97**, 241413 (2018).

[49] S. Sun, H. Kim, G. S. Solomon, and E. Waks, Phys. Rev. Applied **9**, 054013 (2018).

[50] D. D. Sukachev, A. Sipahigil, C. T. Nguyen, M. K. Bhaskar, R. E. Evans, F. Jelezko, and M. D. Lukin, Phys. Rev. Lett. **119**, 223602 (2017).

[51] R. E. Evans, M. K. Bhaskar, D. D. Sukachev, C. T. Nguyen, A. Sipahigil, M. J. Burek, B. Machielse, G. H. Zhang, A. S. Zibrov, E. Bielejec, H. Park, M. Lončar, and M. D. Lukin, Science **362**, 662 (2018).

[52] P. C. Maurer, G. Kucsko, C. Latta, L. Jiang, N. Y. Yao, S. D. Bennett, F. Pastawski, D. Hunger, N. Chisholm, M. Markham, D. J. Twitchen, J. I. Cirac, and M. D. Lukin, Science **336**, 1283 (2012).

[53] Lacour, S., Eisenhauer, F., Gillessen, S., Pfuhl, O., Woillez, J., Bonnet, H., Perrin, G., Lazareff, B., Rabien, S., Lapeyrère, V., Clénet, Y., Kervella, P., and Kok, Y., A&A **567**, A75 (2014).

[54] S. T. Ridgway, *Visibility, Optical Tolerances, and Error Budget*, Tech. Rep. 2 (Center for High Angular Resolution Astronomy, 1994).

[55] H. Bernien, B. Hensen, W. Pfaff, G. Koolstra, M. S. Blok, L. Robledo, T. H. Taminiau, M. Markham, D. J. Twitchen, L. Childress, and R. Hanson, Nature **497**, 86 (2013).

[56] H. Kaushal, V. K. Jain, and S. Kar, "Free-space optical channel models," in *Free Space Optical Communication* (Springer India, New Delhi, 2017) pp. 41–89.

[57] S. Muralidharan, L. Li, J. Kim, N. Lütkenhaus, M. D. Lukin, and L. Jiang, Scientific Reports **6** (2016).

[58] B. Koehler, *VLTI Concept & technical aspects*, European Southern Observatory, Garching (2001).

[59] C. W. Helstrom, Journal of Statistical Physics **1**, 231 (1969).